Asiatic Citrus Canker: Spatial and Temporal Spread in Simulated New Planting Situations in Argentina

T. R. Gottwald, R. G. McGuire, and S. Garran

Research plant pathologist, Agricultural Research Service, U.S. Department of Agriculture, Orlando, FL 32803; assistant plant pathologist, University of Florida, Institute of Food and Agriculture Sciences, Lake Alfred, FL 33850; Instituto Nacional de Tecnologia Agropecuaria, Concordia, Entre Rios, Argentina.

The authors wish to express their appreciation to numerous personnel at the Instituto Nacional de Tecnologia Agropecuaria-Estacion Experimental Agropecuaria facility in Concordia, Argentina, for providing the land and helping to establish and maintain the research plots. We also wish to express our gratitude to Alice Dow, Connie Ferriola, Cesar Hurtado, Mario Scheifler, and Victor Scheifler for technical assistance and to L. W. Timmer and J. H. Graham for their efforts in administrating the USDA/Office of International Cooperation and Development grant which made this study possible.

Accepted for publication 10 December 1987.

ABSTRACT

Gottwald, T. R., McGuire, R. G., and Garran, S. 1988. Asiatic citrus canker: Spatial and temporal spread in simulated new planting situations in Argentina. Phytopathology 78:739-745.

Single replant trees, one each of cultivars Marsh grapefruit and Valencia orange, were inoculated with a rifampicin-resistant strain of *Xanthomonas campestris* pv. *citri*. These inoculated trees were planted in the center of two plots each consisting of 187 trees (approximately 1.0 m tall) of the corresponding cultivar. Spread of epiphytic bacteria from the focal trees was monitored by immunofluorescence microscopy, and incidence of diseased trees was determined by observing visual symptoms. Disease was first detected 49 days after diseased trees were placed in the field. Initial disease spread was highly directional and associated with high winds and blowing rain in mid-January. Subsequent spread was less rapid and generally nondirectional. Monomolecular, logistic, and Gompertz models were tested for goodness-of-fit to disease progress data. The Gompertz model was superior in describing the increase of citrus canker over time. The rate of disease increase (Gompertz rate parameter, k) was 0.005 and 0.009 per day for orange and grapefruit plots, respectively. Disease gradients of $-\ln(-\ln(y)) = a - b \log_{10} m$, where y = disease severity (%) and m = distance from the disease focus of infection in meters, varied over time from -0.713 to -1.237 and from $+0.048$ to -1.856 for orange and grapefruit plots, respectively. The rate of disease progress also was affected by disease-induced defoliation. Disease gradients steepened over time as a result of disease-induced defoliation that often exceeded 90% on individual trees.

Citrus bacterial canker (CBC) caused by *Xanthomonas campestris* pv. *citri* (Hasse) Dye (XCC) occurs in many citrus-growing countries worldwide (13–15). The bacterium causes lesions on foliage, green wood, and fruit of numerous citrus cultivars and citrus relatives (20). Asiatic citrus canker (CBC-A) is widely distributed worldwide and its causal organism, XCC-A, has the widest known host range of any CBC bacterium. In 1984, an outbreak of a CBC-like disease occurred in a nursery in Polk County, FL. Since that time, the disease has been confirmed at 20 locations in the central Florida area, mostly in citrus nurseries and on immature trees (24,25). The disease organism, isolated in Florida, was serologically and genetically distinct from XCC-A and all other XCC strains (5,6,9–11,16,17). In addition, disease symptomatology was unique. Leaf lesions were usually flat (rather than erumpent and raised as is typical with CBC-A) and water-soaked with chlorotic halos (4). In 1986, during the enhanced grove and nursery surveys conducted by the Florida Department of Plant Industry in an attempt to locate and eradicate trees with the nursery CBC-like disease, CBC-A was discovered at five sites in Pinellas and Manatee counties in Florida. The present threat of both CBC-A and the new nursery CBC-like disease in Florida has created an urgency to obtain as much information as possible about these diseases.

Although CBC-A previously had been eradicated from Florida by 1927 by the destruction of about 20 million nursery and grove trees, the epidemiology of the disease was not studied. Therefore, information on field epidemiology of CBC must be extrapolated from CBC-A epidemics that have occurred elsewhere. Studies of these epidemics found that temperatures between 20 and 35 C with an optimum of 30 C combined with free moisture were conducive to infection and disease development of CBC-A (13,21,23). Dissemination of XCC-A and subsequent incidence of CBC-A are directly related to windblown rain, especially at wind speeds in excess of 8 m/sec (23,26,27). Bacterial concentrations in rainwater collected from foliage infected with CBC-A were as high as 10^5 to 10^6 cfu/ml and were 10^4 cfu/ml in rainwater collected under diseased plants (7). Detectable levels of XCC-A bacteria have been found in rainwater up to 32 m from diseased foliage (7).

Rates of disease increase (k) of CBC-A in groves in Argentina were calculated, from linearized Gompertz transformed data, to be 0.04–0.06, 0.1, 0.18, and 0.13–0.24 from mandarin, satsuma, navel, and sweet orange, respectively (8). Rates of disease increase were affected by scion/rootstock combinations (1). Slopes of Gompit (y) vs. $\log_{10} m$ linearized disease gradients ranged from -0.21 to -4.13; however, discrete initial foci of inoculum were not determined (7).

The spatial and temporal dynamics of Asiatic citrus canker originating from a known, discrete source of inoculum within a solid block of a single cultivar have not been investigated previously. This information is essential if we are to understand the potential for epidemic development in commercial citrus groves. The purpose of this study was to investigate the dynamics of the epiphytic XCC populations on the phylloplane and to quantitate the spatial and temporal progress of CBC-A in citrus replant situations with a known, focal source of inoculum.

MATERIALS AND METHODS

All experiments were performed under new grove conditions. Two plots, each consisting of 187 1-m trees of *Citrus paradisi* Macf. 'Marsh' and *C. sinensis* (L.) Osbeck 'Valencia,' were established about 60 m apart at the Instituto Nacional de Tecnologia Agropecuaria Agricultural Experiment Station in Concordia, Entre Rios, Argentina. Trees were planted about 76 cm (30 in.) apart in three concentric circles with radii of 4.6, 9.2, and 13.8 m (15, 30, and 45 ft) from a central focal tree inoculated with XCC.

The 4.6-m circle interval was selected because in Florida resets and new groves often are planted with the shortest dimension between trees of 4.6 m. The rationale for concentric circles was to ensure the availability of susceptible host plant material at regular intervals from a focal point of disease regardless of direction of wind or rain splash. Plots were irrigated by overhead sprinklers every other day for 30 min.

Inoculum and focal plant preparation. Strains of XCC-A were obtained by macerating lesions taken from diseased leaves of *C. paradisi* in 1–2 ml distilled water, streaking the macerate on semiselective media, and incubating at 28 C for 3 to 4 days (20). To develop an antibiotic-tolerant strain of XCC-A, bacteria from individual colonies were suspended in 5 ml sterile water, and 0.5 ml of the bacteria was spread onto nutrient agar. A few grains of rifampicin (3-[4-Methylpiperazinyliminomethyl]rifamycin) (Sigma Chemical Co., St. Louis, MO) were sprinkled onto the agar surface. After 72 hr, a lawn of bacteria developed, with a clear zone surrounding the grains of rifampicin in which only a few individual bacterial colonies occurred. Individual colonies were streaked onto nutrient agar amended with 100 μg/ml of rifampicin. Individual colonies from rifampicin-amended media were tested for pathogenicity by suspending cells in sterile distilled water, adjusting the suspension to a barely visible turbidity (about 10^5 to 10^6 cfu/ml), and infiltrating a small volume of each suspension by syringe into seedling leaves of *C. paradisi* 'Duncan.' The strain that elicited the most severe disease response (LTV5) was reisolated and maintained in sterile tap water at 5 C.

Inoculum was prepared by flooding 48-hr-old nutrient agar plates containing strain LTV5 with tap water and bringing the bacteria into suspension with a bent glass rod. The bacteria from each of several plates were collected in a common flask. The flask was shaken vigorously to suspend the cells evenly, and the suspension was adjusted visually to a moderately turbid concentration (about 10^7 to 10^8 cfu/ml). A further diluted suspension, about 10^4 cfu/ml, was used to inoculate by infiltration 150 leaves of each of two citrus trees, one Valencia orange and one Marsh grapefruit. Subsequently, a portion of concentrated suspension, about 10^7 to 10^8 cfu/ml, was atomized onto adaxial and abaxial leaf surfaces until runoff. Inoculated plants were covered with a plastic bag to retain foliar moisture and were maintained under ambient greenhouse conditions for 5 days. Bags were then removed, and symptoms were allowed to develop for 30 days before the trees were transplanted to the field plot. Because of the differing amount of susceptible tissue on each plant at the time of inoculation, the orange focal tree had a higher initial disease incidence than the grapefruit focal tree.

Sampling design and procedure. Two transect lines were established through each plot. The first line ran from north to south through the focal plant in the center of each plot. This transect was parallel to the direction of the prevailing wind. A second transect line was perpendicular to the first, from west to east, through the focal plant. Those trees closest to the lines in each concentric circle were designated sampling points. Two additional trees were designated sampling points in each concentric circle on the downwind (north) side of the plot to ensure detection of any bacterial spread in that direction. In the 9.2-m and 13.8-m radii concentric circles, the two additional trees were one and two trees away from the designated sample tree, respectively. This formed a uniform fan-shaped sampling pattern downwind from the focal tree. Two asymptomatic leaves, one from each of the sides nearest and farthest from the focal tree, were taken from each of the designated trees approximately every three weeks.

Determination of epiphytic bacteria. Immunofluorescence microscopy (IF) was used to detect epiphytic XCC-A from leaves. On each sampling day, two 5.0-mm leaf disks were excised with a No. 2 cork borer and removed from each of two asymptomatic leaves from each sample tree. These were pooled by tree and fixed in 3% glutaraldehyde in 0.066 M phosphate buffer, pH 6.8, for at least 48 hr. The leaf disks were then rinsed twice in phosphate-buffered saline containing 0.2% sodium azide. Disks were minced in one to two drops of distilled water with a single-edged razor blade. Tissue and water were then transferred to a 12 × 75 mm test tube, diluted with 2 ml distilled water, and vigorously mixed for about 15 sec on a vortex mixer. The course material was allowed to settle; then the supernatant and any bacteria were drawn into a pipette and transferred to a 10-ml syringe. The solution was forced through a double filtration apparatus consisting of a 5.0-μm nitrocellulose prefilter to remove large cell debris and then a 0.2-μm, black, polycarbonate membrane filter to trap any bacteria. The polycarbonate filter was removed, placed in a 35 × 10 mm petri dish, and stained with three to four drops of 1:20 dilution of tetramethylrhodamine isothiocyanate conjugated with IgG antibody prepared against XCC-A for 1 to 2 min. The excess stain was removed with a pipette. The polycarbonate filter was mounted on a glass microscope slide with Aqua Mount (Lerner Laboratories, New Haven, CT) and covered with a 22 × 30 mm nonfluorescent glass coverslip. The mounts were allowed to cure overnight, sealed with clear fingernail polish, and examined at 1,000× under oil with a Zeiss Universal compound microscope with epifluorescence for the presence of XCC-A bacteria (3).

To test for the presence of XCC-A on foliage of diseased citrus and nondiseased citrus, and on weeds in the near vicinity, sample leaves were removed from the plants and shaken 30 min in 0.075 M phosphate buffer, pH 6.8 (10 ml/leaf) on a shaker. Both the wash water and serial dilutions were spread on semiselective media (0.1 ml/plate) and incubated at 28 C for 4 days (20). To determine if the bacteria isolated were the same strain placed in the plots at the beginning of the experiment, colonies were occasionally transferred to semiselective media amended with 100 ppm rifampicin.

Analysis of disease progression. Disease was assessed visually for each tree in both plots on each sampling day as the percentage of diseased leaves per tree. The leaves on each tree with at least one lesion were counted, and the number was divided by the estimated total number of leaves on the tree. Disease progress was analyzed for each plot separately. In addition, each plot was partitioned into four sectors, the common corner of which was the central focal tree of infection. In this way, disease progress could be analyzed for each potential direction of disease spread: northeast, northwest, southwest, and southeast. Data were first taken on 24 December (day 1) when the focal trees were first placed in the plots. Seven more sampling dates were included in the analysis, the last being 13 July (day 220) and 8 August (day 228) for the Valencia orange and Marsh grapefruit plots, respectively. The epidemic had reached an asymptote at this time. The goodness-of-fit of the linear forms of the monomolecular, logistic, and Gompertz models (2,18) to disease progress data was examined by least squares regression analysis. To test the appropriateness of each model, standardized residual plots were examined (19). To test the efficiency of each model for describing disease progress within each plot, predicted values were detransformed and correlated with observed, nontransformed values. Models that are superior have larger correlation coefficients (12). Disease gradients were described for each plot, or directional sector of each plot, by the slope (b) of the transformed disease proportion (y) regressed on the $\log_{10}$ of the distance from the focal tree (7).

Ordinary runs and original doublet analyses were used to determine the aggregation of diseased trees within each concentric ring (19). Analysis was performed by dividing each plot into three subplots of 31, 62, and 92 contiguous trees corresponding to the 4.6-, 9.2-, and 13.8-m rings of trees, respectively. A nonrandom pattern or "clustering" of diseased or healthy trees was assumed if the expected number of runs was less than, or the expected number of doublets exceeded, the observed values at $P = 0.05$.

RESULTS

Epiphytic bacteria were first detected by IF on 20 January (day 27) in the grapefruit circle plot (GCP). Epiphytic XCC-A bacteria were detected on sampled plants 4.6 and 9.2 m north of the focal plant. Detection of epiphytic populations of XCC-A in the orange circle plot (OCP) did not occur until early May (day 136), at which time the disease was well established in both plots. At this time, epiphytic XCC-A populations were found on grapefruit trees in the

GCP predominantly in the northern direction. Epiphytic populations of XCC-A continued to increase in the GCP throughout the remainder of the season, occasionally in concentrations of 117–263 cells/cm^2 leaf surface area, but were only occasionally detected on orange foliage in the OCP and never in numbers greater than 18 cells/cm^2 as determined on semi-selective media (*unpublished*).

Isolations from diseased and nondiseased foliage made during the season and at the end of the season in both plots yielded rifampicin-tolerant isolates of XCC-A only. Therefore, we presume that bacteria from exogenous sources did not invade the plots. Antibiotic-tolerant XCC-A bacteria also were recovered from leaf washings of weeds, both within and up to 5 and 10 m from the northern edge of the OCP and the GCP, respectively.

Analysis of disease progression. The Gompertz model gave the best fit to progress of disease over time for both whole plots (Table 1). Correlation analysis of detransformed predicted values with nontransformed observed values resulted in a slightly higher coefficient of correlation by the monomolecular model for the GCP plot only. The monomolecular model was, however, the poorest model in explaining the variation by linear regression. The Gompertz model was therefore considered the better model overall to describe disease progress within both plots and was used for direct comparisons.

Disease proportion, assessed as the percentage of diseased leaves per tree, was considerably greater at the onset of the epidemic on the Valencia OCP focal tree than on the Marsh GCP focal tree: 0.95 vs. 0.043, respectively. At midseason, the percentage of diseased foliage increased on the GCP focal tree and decreased on the OCP focal tree (Fig. 1A and B). First detection of disease spread in both plots was simultaneous, about 49 days after diseased focal trees were placed in both the OCP and the GCP. Disease incidence was detected to the northeast in both plots: 9.2 and 13.8 m from the focal trees in the OCP and the GCP, respectively (Fig. 2A and B). Although both initial disease incidence and initial disease severity were lower in the GCP than the OCP, the disease increased in severity and intensified in incidence more rapidly in the GCP (Figs. 1C and D, 2C and D). Final disease incidence was 86 and 97%, respectively, for the OCP and the GCP. Final disease incidence of the individual directional sectors was 91, 74, 83, and 98%, and 100, 87, 100, and 100% for the northeast, southeast, southwest, and northwest sectors of the OCP and the GCP, respectively. The nondirectional rate of disease increase measured as the Gompertz rate parameter (k) was 0.005 and 0.009 for the entire OCP and the entire GCP, respectively. Rates of disease increase were highest in the northeast and lowest in the southeast sectors in both plots and ranged from 0.001 to 0.006 and from 0.004 to 0.011 for the OCP and the GCP, respectively.

The gradients of disease from the central focal plant to the edge of the plots are represented by the linear regression of the Gompertz-transformed disease proportion by the log of the distance from the focal tree (Fig. 3). Coefficients of determination (R^2) were generally high (>0.70–0.99) except in a few cases early in the epidemic (Table 2). Initial disease gradients were steeper in the OCP than the GCP, indicating that a higher concentration of disease occurred early in the season near the focus in the OCP and that disease distribution was more diffuse in the GCP during the same period. Disease gradients in the OCP began to flatten through the 114-day sampling period, started to steepen from day 114 to day 162, then flatten again on the last sampling day (Fig. 3A). The disease gradient in the GCP was initially flat on the first sampling date (day 43) because the disease proportion on the focal tree was low and those plants to the northeast, infected from the initial spread of the disease, were similar in severity to the focal plant (Fig. 3B). The GCP disease gradient began to steepen by day 73 as the number of diseased plants and their severity increased.

TABLE 1. Analysis of disease increase of Asiatic citrus canker in simulated new plantings in Argentina

	Monomolecular model			Logistic model			Gompertz model[c]		
Plot[a]	R^2[b]	Slope ± standard error	r of observed[c] vs. predicted	R^2	Slope ± standard error	r of observed vs. predicted	R^2	Slope ± standard error	r of observed vs. predicted
OCP	0.865	0.0008 ± 0.0001	0.925	0.898	0.0178 ± 0.0025	0.895	0.907	0.0052 ± 0.0007	0.944
GCP	0.716	0.0017 ± 0.0004	0.855	0.818	0.0340 ± 0.0065	0.625	0.850	0.0092 ± 0.0016	0.773

[a] OCP = Valencia orange circle plot; GCP = Marsh grapefruit circle plot. Plots were laid out in three concentric circles of trees at 4.6-, 9.2-, and 13.8-m radii from a central focal tree inoculated with *Xanthomonas campestris* pv. *citri*.
[b] Coefficients of determination (R^2) and slopes (b) were estimated by regressing transformed disease percentages over time. Disease percentages were transformed by $\ln(1/(1-y))$, $\ln(y/(1-y))$, and $-\ln(-\ln(y))$ (monomolecular, logistic, and Gompertz transformations, respectively).
[c] Predicted values were detransformed and regressed against original observations to test the models.

TABLE 2. Comparison of citrus canker disease gradients from point sources in Valencia orange and Duncan grapefruit replant plots in Argentina

		Nondirectional		Downwind		Upwind		Ratio (Nondirectional/ downwind)[d]
Plot	Day[a]	b[b]	c.f.[c]	b	c.f.	b	c.f.	
Valencia orange	43	...	...	...	...	...	...	...
	73	−1.183	−0.990	−1.384	−0.995	...	...	0.85
	92	−0.926	−0.982	−1.317	−0.974	−0.552	−0.592	0.70
	114	−0.713	−0.834	−1.000	−0.987	−1.283	−0.991	0.71
	135	−0.920	−0.987	−0.941	−0.954	−1.829	−0.971	0.98
	162	−1.237	−0.972	−0.876	−0.998	−2.458	−0.941	1.41
	220	−0.981	−0.938	−0.022	+0.053	−2.536	−0.933	44.59
Marsh grapefruit	43	+0.048	+0.073	+0.216	+0.236	...	...	0.22
	73	−0.714	−0.982	−0.739	−0.950	...	...	0.97
	92	−0.454	−0.915	+0.065	+0.215	−1.275	−0.908	6.98
	114	−1.362	−0.912	−0.995	−0.733	−1.939	−0.929	1.37
	135	−1.705	−0.935	−1.750	−0.913	−2.379	−0.989	1.87
	172	−1.856	−0.974	−1.378	−0.842	−2.601	−0.999	1.35
	228	−0.723	−0.757	−0.942	−1.000	−1.030	−0.680	0.72

[a] Number of days after the infected focal tree was placed in the plot.
[b] b = slope of Gompertz-transformed disease rating vs. $\log_{10}$ distance.
[c] c.f. = correlation coefficient.
[d] Downwind direction was northeast; upwind direction was southeast for purposes of analysis.

The GCP disease gradient fluctuated throughout the remainder of the season, reaching maximum steepness by day 172 and flattening again by the final sampling date, day 228 (Fig. 3B).

The directional spread of citrus canker was to the northeast or downwind direction early in the season; the ratio of the slope of the disease gradient of the whole plot to that of the downwind direction was less than 1.0 (10) (Table 2). Secondary spread within the plots occurred during midseason in the GCP and in late season in the OCP, when the ratio on the slopes approached or exceeded 1.0. In general, disease continued to develop most heavily in the northeast, downwind direction, as shown by the higher upwind disease gradient slopes (Table 2).

Aggregation of diseased trees was demonstrable in the two innermost rings of trees in the OCP and in all three rings of the GCP trees on day 49 (12 February). Tests continued to negate the assumption of randomness of diseased trees in all tree rings throughout both plots for the remainder of the epidemic. As suggested by Madden et al (19), the ordinary runs method gave more satisfactory predictions of randomness than the original doublets procedure. The two methods were in disagreement, especially at higher disease incidence levels late in the epidemic (Table 3).

DISCUSSION

Because direct isolation of XCC-A from leaf washings produced only the rifampicin-tolerant XCC-A isolates, it was presumed that no exogenous sources of inoculum were interfering with disease progression within the plots. Thus, the central focus trees were assumed to be the sole source of inoculum within the plots.

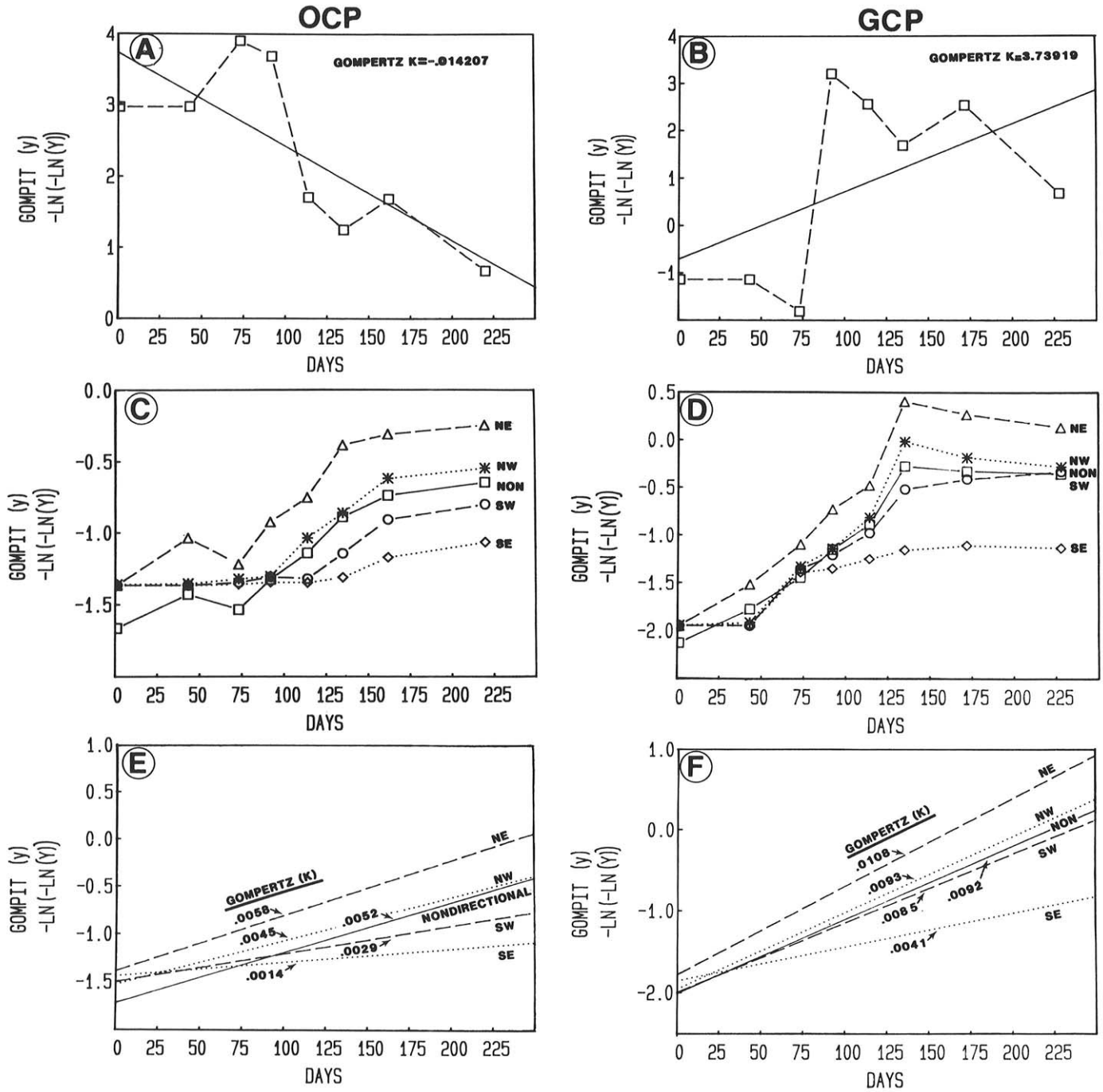

Fig. 1. Disease progress of Asiatic citrus canker in new grove simulations of Valencia orange (OCP) and Marsh grapefruit (GCP). **A and B,** Disease progress on centrally located focal trees in each plot. Dashed line is actual disease progress. Solid line represents linear regression of disease progress. **C and D,** Disease progress curves over time for the plot as a whole (NON = nondirectional) and for four directional quadrants (NE, NW, SE, and SW). **E and F,** Linear regression approximations of Gompertz-transformed disease progress curves for nondirectional and directional quadrants.

Phylloplane populations of XCC-A occurred more often and in greater numbers on grapefruit foliage than on orange foliage. Higher leaf surface populations on grapefruit may indicate that this host is more susceptible to CBC-A than is sweet orange (22). Higher surface populations would result in more available inoculum for splash dissemination which would account, at least in part, for the higher rates of disease increase in the GCP compared to the OCP (Fig. 1E and F).

In most cases, disease gradients flatten over time in response to and increase in the number of diseased plants at the periphery of the plot. This is usually due to secondary spread within the plots and a general increase in disease severity of plants at some distance from the focus (10). The steepening of the disease gradient over time in groves infested with citrus canker has been previously reported (7). It was felt that localized secondary spread to adjacent trees near the focus was strong, resulting in steeper gradients. In the present study, disease gradients fluctuated over the season. Because trees used in this study were only about 1 m tall, disease intensity often surpassed 90% and was frequently accompanied by severe stem infections and defoliation. Trees defoliated during the growing season soon set a new flush of growth, which subsequently became diseased. This cyclic defoliation in response to severe disease and refoliation with young, undiseased foliage resulted in an effective decrease in disease proportion. This, combined with the subsequent infection of new foliage, causing an increase in disease proportion, resulted in the fluctuations observed in the disease gradients and possibly the disease progress curves over time. Citrus canker increased more rapidly in the grapefruit planting than in the orange planting, reflecting the greater susceptibility of grapefruit to the disease (22). The more intense disease buildup in the GCP caused more intense cyclic defoliation and refoliation in that plot as demonstrated by the greater fluctuations in disease gradient over time (Fig. 3B). The ratio of the slope of the disease gradients of the entire plot to the downwind direction (dnd/ddw) is indicative of directional spread of the disease by wind (10). Disease spread in the downwind direction should result in a flatter slope of the disease gradient in that direction and, thus, a ratio of less than 1.0. As localized spread from secondary foci occurs or fluctuates in direction, the ratio approaches or exceeds 1.0. The ratio of the nondirection to the downwind disease gradient slopes was confounded by these disease fluctuations, as evidenced by the end-of-season ratio in both plots (Table 2). Even though these fluctuations occurred, the upwind disease gradient slope was usually greater than the downwind slope during most sampling days (Table 2).

As expected, tests for randomness of disease incidence

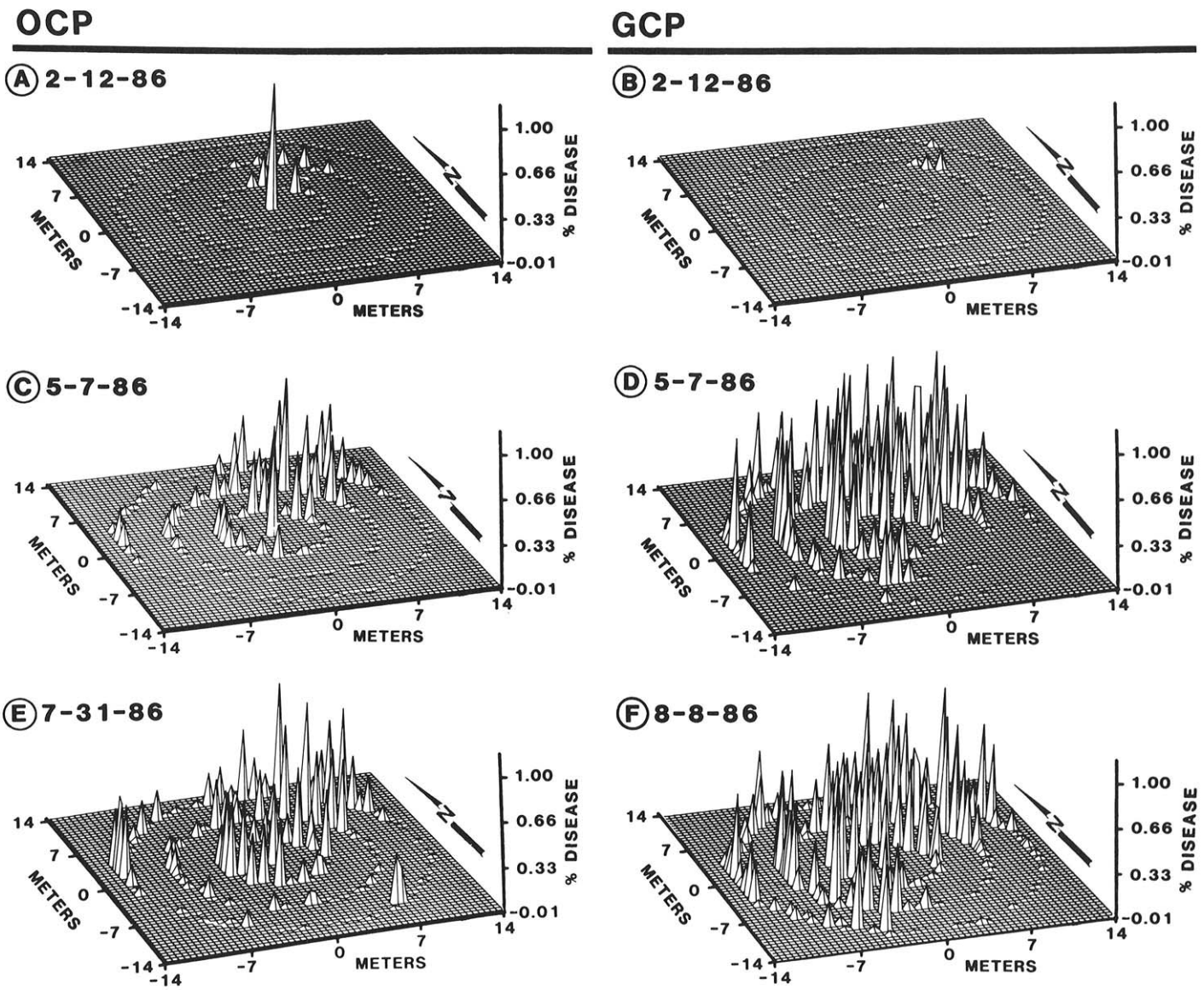

Fig. 2. Three-dimensional response surface representations of disease development and spatial spread of Asiatic citrus canker in Valencia orange (OCP) and Marsh grapefruit (GCP) over time. Plots established 24 December 1985. Note initial spread toward the northeast in both plots and subsequent general disease spread.

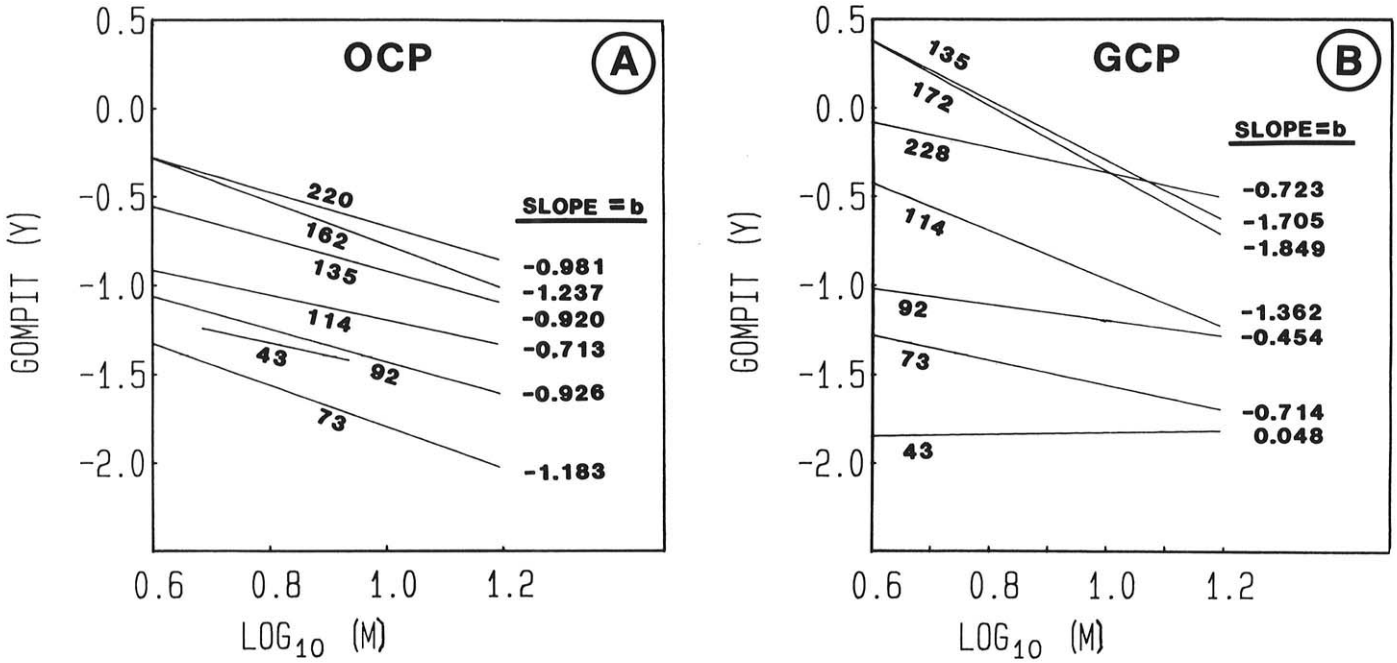

Fig. 3. Disease gradients of Asiatic citrus canker in new grove simulations of Valencia orange (OCP) and Marsh grapefruit (GCP). Lines represent linear regressions of Gompertz-transformed disease percentages versus the $\log_{10}$ of the distance from the focus of disease. The individual days for which the data were regressed are shown under each line. Note increases and decreases in slopes over time due to intense disease buildup followed by defoliation (see Discussion).

TABLE 3. Example of ordinary runs and original doublet analysis of orange and grapefruit replant plots infected with Asiatic citrus canker 9.2 m[a] from focus of infection

Plot	Date	Analysis[b]	Disease percentage	Observed	Expected	Sd	Z[c]	P[d]
Valencia orange								
	2-12-86	U	14.8	4	16.34	1.92	−6.18	0.000
		D		7	1.18	1.07	5.45	0.000
	3-6-86	U	11.5	2	13.39	1.53	−7.10	0.000
		D		6	0.68	0.81	6.51	0.000
	3-25-86	U	43.5	18	31.10	3.82	−3.30	0.001
		D		18	11.51	3.34	1.95	0.026
	4-16-86	U	58.1	22	30.51	3.74	−2.14	0.016
		D		25	20.66	4.47	0.97	0.166
	5-7-86	U	64.5	14	28.54	3.49	−4.02	0.000
		D		33	25.57	4.97	1.49	0.068
	6-3-86	U	74.2	14	23.62	2.85	−3.19	0.001
		D		39	33.93	5.73	0.88	0.189
	7-31-86	U	87.1	8	13.39	1.53	−3.19	0.001
		D		51	46.92	6.74	0.61	0.271
Marsh grapefruit								
	2-12-86	U	9.7	4	11.84	1.32	−5.55	0.000
		D		4	0.48	0.68	5.14	0.000
	3-6-86	U	24.42	9	23.74	2.85	−5.00	0.000
		D		11	3.34	1.81	4.21	0.000
	3-25-86	U	53.2	19	31.87	3.89	−3.18	0.001
		D		24	17.03	4.06	1.72	0.043
	4-16-86	U	77.4	11	22.68	2.71	−4.12	0.000
		D		43	36.39	5.93	1.11	0.134
	5-7-86	U	90.3	5	11.84	1.32	−4.79	0.000
		D		54	49.68	0.62	0.62	0.268
	6-13-86	U	93.5	3	8.48	0.89	−5.59	0.000
		D		58	53.32	7.18	0.65	0.259
	8-8-86	U	98.4	3	2.97	0.18	3.01	0.001
		D		61	59.03	7.56	0.26	0.394

[a] Although all three distances (4.6, 9.2, and 13.8 m) were tested, only the 9.2-m distance from the focus of inoculum is presented here.
[b] U = ordinary runs analysis, and D = original doublet analysis. Both procedures test for randomness of disease within a population.
[c] Standardized variable large negative numbers indicate clustering with ordinary runs analysis, whereas large positive values indicate clustering with original doublets.
[d] Significance level. Levels less than $P = 0.05$ were considered indicative of clustering of diseased plants.

demonstrated clustering of diseased trees immediately after the first recorded spread of the disease. Early spring rainstorm activity, which stimulated the initial spread of the CBC-A, resulted in considerable clustering of diseased trees, predominantly in the northeasterly direction from the focus. Tests for randomness indicated that this clustering effect remained throughout the remainder of the epidemic and that spread was largely confined to closely neighboring trees.

Early-season spread of CBC-A in the plots appeared to have been the result of rainstorms combined with high winds in mid and late January (days 24 and 37), causing a northeasterly dissemination of XCC-A. In Argentina, citriculturists often refer to these as "canker winds." Subsequent rains in late February and throughout the remainder of the season intensified the disease on individual trees, which often exceeded 90% diseased foliage, and contributed to localized movement to neighboring trees. Undoubtedly, overhead sprinkler irrigation in the plots also intensified the disease and aided dissemination of the pathogen. Even so, the rates of disease increase in the present study of $k = 0.005$ and $k = 0.009$ for the OCP and the GCP, respectively, fell below those ranges previously described even for more susceptible cultivars (7,8).

The amount of CBC-A that developed in the plots during the present season far exceeded that which developed in any of the natural grove situations in the vicinity during the same period of time. Thus, we were successful in creating and maintaining conditions necessary for rapid disease buildup. The previous study was conducted during an intense citrus canker eradication campaign in Argentina (7,8). Disease was more prevalent in commercial plantings than during the present study or during the last several years. In addition, there was no discrete focus of infection in the previous study and, presumably, disease ingress could have occurred from one or more exogenous sources of inoculum. Both of these factors help to explain why the rates of disease increase described here were somewhat lower.

LITERATURE CITED

1. Agostini, J. P., Graham, J. H., and Timmer, L. W. 1985. Relationship between development of citrus canker and rootstock cultivar for young 'Valencia' orange trees in Missiones, Argentina. Proc. Fla. State Hortic. Soc. 98:19-22.
2. Berger, R. D. 1981. Comparison of the Gompertz and logistic equations to describe plant disease progress. Phytopathology 71:716-719.
3. Brlansky, R. H., Lee, R. F., and Civerolo, E. L. 1986. Detection of *Xanthomonas campestris* from citrus by membrane entrapment and immunofluorescence. (Abstr.) Phytopathology 76:1101.
4. Civerolo, E. L. 1984. Bacterial canker disease of citrus. J. Rio Grande Val. Hortic. Soc. 37:127-146.
5. Civerolo, E. L., and Fan, F. 1982. *Xanthomonas campestris* pv. *citri* detection and identification by enzyme-linked immunosorbent assay. Plant Dis. 66:231-236.
6. Civerolo, E. L., and Helkie, C. 1982. Indirect enzyme-linked immunosorbent assay of *Xanthomonas campestris* pv. *citri*. Pages 105-112 in: Proc. Int. Conf. Plant Pathog. Bact. 5th.
7. Danos, E., Berger, R. D., and Stall, R. E. 1984. Temporal and spatial spread of citrus canker within groves. Phytopathology 74:904-908.
8. Danos, E., Bonazzola, R., Berger, R. D., Stall, R. E., and Miller, J. W. 1981. Progress of citrus canker on some species and combinations in Argentina. Proc. Fla. State Hortic. Soc. 94:15-18.
9. Gabriel, D. W. 1985. Four plasmid DNA variants distinguished in 1984 Florida citrus canker epiphytotic. (Abstr.) Phytopathology 75:1320.
10. Gregory, P. H. 1968. Interpreting plant disease dispersal gradients. Annu. Rev. Phytopathol. 6:189-212.
11. Hartung, J. S., and Civerolo, E. L. 1986. Genomic fingerprints of *Xanthomonas campestris* pv. *citri* strains from Asia, South America, and Florida. (Abstr.) Phytopathology 76:1137.
12. Hau, B., and Kranz, J. 1977. Ein verschiedener Transformationen von Befallskurven. Phytopathol. Z. 88:53-68.
13. Koizumi, M. 1977. Relation of temperature to the development of citrus canker in the spring. Proc. Int. Soc. Citriculture 3:924-928.
14. Koizumi, M. 1981. Citrus canker. Pages 8-12 in: Citrus Diseases in Japan. T. Miyakawa and A. Yamaguchi, eds. Japan Plant Protection Assoc.
15. Koizumi, M. 1985. Citrus canker: The world situation. Pages 2-7 in: Citrus Canker: An International Perspective. Proc. Symp. Inst. Food Agric. Sci., Univ. Fla. L. W. Timmer, ed. 28 pp.
16. Lazo, G. R., and Gabriel, D. W. 1987. Pathovars of *Xanthomonas campestris* are distinguishable by restriction fragment length polymorphisms. Int. J. Syst. Bacteriol. (In press)
17. Lazo, G. R., and Gabriel, D. W. 1987. Conservation of plasmid DNA sequences within pathovars of *Xanthomonas campestris*. Phytopathology 77:448-453.
18. Madden, L. V. 1980. Quantification of disease progression. Prot. Ecol. 2:159-176.
19. Madden, L. V., Louie, R., Abt, J. J., and Knoke, J. K. 1982. Evaluation of tests for randomness of infected plants. Phytopathology 72:195-198.
20. McGuire, R. G., Jones, J. B., and Sasser, M. 1986. Tween media for semiselective isolation of *Xanthomonas campestris* pv. *vesicatoria* from soil and plant material. Plant Dis. 70:887-891.
21. Peltier, G. L. 1920. Influence of temperature and humidity on the growth of *Pseudomonas citri* and its host plants and on infection and development of the disease. J. Agric. Res. 20:447-506.
22. Peltier, G., and Frederich, W. J. 1924. Further studies on the relative susceptibility to citrus canker of different species and hybrids of the genus *Citrus*, including the wild relatives. J. Agric. Res. 28:227-239.
23. Reedy, B. C. 1984. Incidence of bacterial canker of citrus in relation to weather. Geobios New Rep. 3:39-41.
24. Schoulties, C. L., Civerolo, E. L., Miller, J. W., Stall, R. E., Krass, C. J., Poe, S. R., and DuCharme, E. P. 1987. Citrus canker in Florida. Plant Dis. 71:388-395.
25. Schoulties, C. L., Miller, J. W., Stall, R. E., Civerolo, E. L., and Sasser, M. 1985. A new outbreak of citrus canker in Florida. (Abstr.) Plant Dis. 69:361.
26. Serizawa, S., and Inoue, K. 1975. Studies on citrus canker III. The influence of wind blowing on infection. Bull. Schizuoka Prof. Citrus Exp. Sta. 11:54-67.
27. Serizawa, S., Inoue, K., and Goto, M. 1969. Studies on citrus canker I. Dispersal of the citrus canker organism. Bull. Schizuoka Prof. Citrus Exp. Sta. 8:81-85.